



PROSPECTS FOR JOINT GW AND HIGH-ENERGY EM OBSERVATIONS OF BNS MERGERS

Barbara Patricelli^{1,2},
Massimiliano Razzano^{1,2} and Giancarlo Cella²

¹University of Pisa

²INFN - Sezione di Pisa

DADI Meeting on Gravitational Waves
May 31- June 1, 2016
Strasbourg

Summary

1 Introduction

2 The method

- NS-NS mergers
- GW detections and sky localizations
- GRB simulations

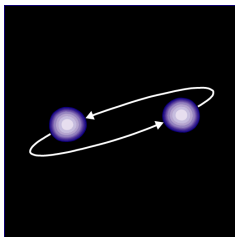
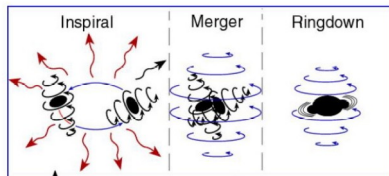
3 Results

- GW detections
- Joint HE EM and GW detections

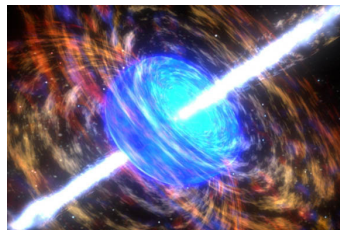
4 Conclusions and future developments

GW150914: first direct observation of Gravitational Waves from a binary BH merger!

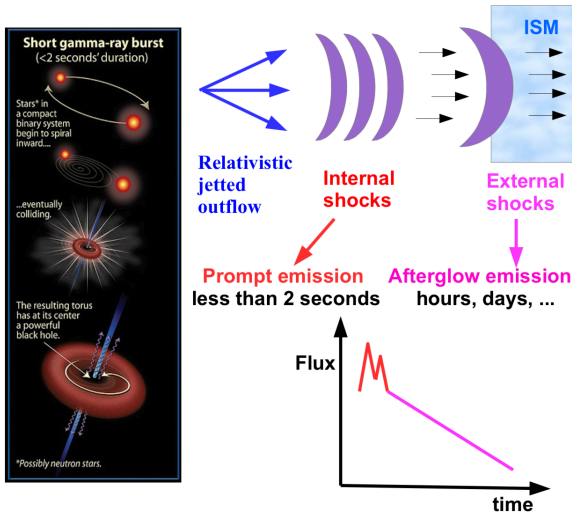
Other promising sources for the next GW detections by Advanced LIGO and Advanced Virgo are **mergers of NS-NS and NS-BH systems**



NS-NS and NS-BH mergers are expected to be associated with short GRBs



Short GRBs



joint GW and EM detections

Two possible scenarios:

- **EM follow-up:** a GW event is detected and an alert is sent to EM telescopes, that start looking for an EM counterpart
- **Externally-triggered GW search:** an EM transient event is detected and GW data are analyzed to look for possible associated GW events.

We focus on:

- Large FOV telescopes:
 - higher probability of detecting a transient source in the monitored portion of sky
 - good coverage of the large GW error boxes (tens to hundreds of square degrees)
- γ -ray telescopes:
 - γ -ray sky less “crowded” \Rightarrow clearer association of an EM transient to the GW event

Among the various γ -ray observatories, **Fermi** is one of those that better combines huge sky and energy coverage.

The Fermi mission



Two instruments:

- **GBM**

- **Energy range:** 8 keV to 40 MeV
- **FOV:** ~ 9.5 sr
- **Sky localization:** overall median error for short GRBs of 8°

- **LAT**

- **Energy range:** 20 MeV to 300 GeV
- **FOV:** ~ 2.4 sr
- **Sky localization:**
 $r_{68} \sim 0.8^\circ$ at 10 GeV on-axis

if GBM detects a GRB above a fixed threshold*, *Fermi* automatically slews to move the GRB into the LAT FOV

* The on-board trigger threshold is ~ 0.7 photons $\text{cm}^{-2} \text{s}^{-1}$

Step 1: simulation of the NS-NS mergers

NS-NS mergers

- NS-NS merger rates are dominated by the contribution from Milky Way-like galaxies (see e.g. O'Shaughnessy et al. 2010)
- Maximum distance considered: 500 Mpc
- $\rho_{galaxies} = 0.0116 \text{ Mpc}^{-3}$ (Kopparapu et al. 2008)
- Simulated galaxies are uniformly distributed in volume
- Merging systems: Synthetic Universe (Dominik et al. 2012)
- Bimodal distribution in metallicity: half at $Z=Z_{\odot}$ and half at $Z=0.1 \cdot Z_{\odot}$ (Panter et al. 2008)
- Merger rates: (Dominik et al. 2012)
 - Reference model: Standard Model B
 - "Optimistic" models: V12A ($Z=Z_{\odot}$) and V2A ($Z=0.1 \cdot Z_{\odot}$)
 - "Pessimistic" models: V12B ($Z=Z_{\odot}$) and V1B ($Z=0.1 \cdot Z_{\odot}$)
- 1000 realizations, each one for a 1 year observing period

Step 2: GW detections and sky localizations

GW signals

- We assume non-spinning systems
- Random inclination of the orbital plane θ with respect to the line of sight
- TaylorT4 waveforms (Buonanno et al. 2009)

GW detections

- Detector configurations (aLIGO and AdV): 2016-2017 and 2019+ (design) (Abbott et al. 2016)
- Independent duty cycle of each interferometer: 80 % (Abbott et al. 2016)
- Matched filtering technique (Wainstein 1962)
- trigger: at least 2 detectors
- Combined detector SNR threshold: 12
- GW localization with BAYESTAR (Singer et al. 2014)

Step 3: GRB simulations - the prompt emission

Assumptions:

- All the BNS mergers are associated to a short GRB;
- The prompt emission can be observed only if the GRB is on-axis ($\theta \leq \theta_j$);
(The GRB prompt emission is constant within the jet angle θ_j , zero outside)
- GRB jet opening angles: $0.3^\circ \leq \theta_j \leq 30^\circ$
(Panaitescu et al. 2011, Rezzolla et al. 2011, Coward et al. 2012)
- “fiducial” θ_j : 10° (see Duffell et al. 2015)

Detection with *Fermi*/GBM

- *Fermi*/GBM FOV: 9.5 sr
- GBM duty cycle: 50 %
- *Fermi*/GBM sensitivity vs GRB brightness?

Step 3: GRB simulations - the prompt emission

Brightness: 64-ms peak photon flux P_{64} from the prompt emission in the 50-300 keV energy band

$$L[1\text{keV} - 10\text{MeV}] = 4\pi D_L^2 \frac{\int_{1\text{keV}}^{10\text{MeV}} EN(E)dE}{\int_{50\text{keV}(1+z)}^{300\text{keV}(1+z)} N(E)dE} P_{64},$$

Lowest brightness measured by Fermi/GBM

- $P_{64,\text{Min}}^{\text{meas}} = 0.75 \pm 0.25 \text{ ph/cm}^2/\text{s}$

Lowest expected brightness for the simulated short GRBs

- Minimum L : $2 \cdot 10^{50} \text{ erg/s}$ (lowest luminosity of short GRBs with known redshift)
- Maximum distance: 500 Mpc ($z \sim 0.12$)
- $N(E)$: Band function (with the typical parameters of Fermi/GBM short GRBs)

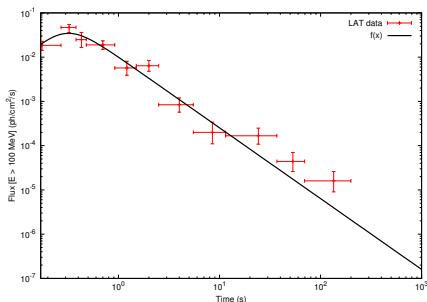
$$\Rightarrow P_{64,\text{Min}} \sim 5 \text{ ph cm}^{-2} \text{ s}^{-1} > P_{64,\text{Min}}^{\text{meas}}$$

\Rightarrow GBM is sensitive enough to detect all the GRBs in our sample

Step 3: GRB simulations - the afterglow emission

GRB 090510 as a prototype:

unique short GRB to show an extended emission (up to 200 s) at high energies (up to 4 GeV), as detected by Fermi-LAT (Ackermann et al. 2010, De Pasquale et al. 2010)



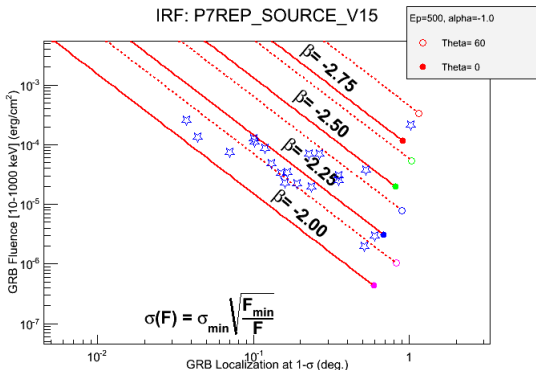
$$F(t) = A \frac{(t/t_{\text{peak}})^\alpha}{1 + (t/t_{\text{peak}})^{\alpha+\omega}}$$

Fixing $\alpha = 2$ as required by the standard afterglow theory (Sari et al. 1999), we found

- $A = 0.07 \pm 0.01 \text{ ph cm}^{-2} \text{ s}^{-1}$
- $\omega = 1.60 \pm 0.15$
- $t_{\text{peak}} = 0.301 \pm 0.04 \text{ s}$
(see also Ghirlanda et al. 2010)

We simulate the GeV afterglows by re-scaling this light curve to take into account the distance of the sources with respect to GRB 090510; for off-axis sources we further correct the light curve for the beaming angle, considering a continuous evolution of Γ .

Step 3: GRB simulations - the afterglow emission



http://www.slac.stanford.edu/exp/glast/groups/canda/archive/p7rep.v15/lat_Performance.htm

- We extrapolated this sensitivity to the energy range 0.1-300 GeV
- We estimated the integration time t_f needed for the simulated GRBs to have a fluence equal to the Fermi-LAT sensitivity; we choose the value of sensitivity corresponding to a GRB localization of 1 deg, for $\beta=-2$.

Results: GW detections

Configurations	Work	Number of BNS detections (yr^{-1})	% of BNS with Loc. $\leq 5 \text{ deg}^2$	% of BNS with Loc. $\leq 20 \text{ deg}^2$	% of BNS with Loc. $\leq 100 \text{ deg}^2$	% of BNS with Loc. $\leq 1000 \text{ deg}^2$
2016-2017	This work	0.1 (0.002 - 1.5)	3	9	16	70
	Singer et al. 2014 ¹	1.5	2	8	15	-
	Abbott et al. 2016	0.006-20	2	14	-	-
2019+ (design)	This work	2.1 (0.08 - 30)	5	21	50	90
	Abbott et al. 2016	0.2-200	> 3-8	> 8-30	-	-

¹These estimates refer to the 2016 scenario.

Results: joint HE EM and GW detections - prompt emission

θ_j	EM	EM and GW	EM and GW
deg	yr^{-1}	2016-2017 yr^{-1}	design yr^{-1}
0.3	0.045	$< 10^{-3}$	0.008
	$< 10^{-3} - 0.525$	$< 10^{-3} - 0.003$	$< 10^{-3} - 0.068$
10	1.256	0.010	0.2130
	0.021 - 18.201	$< 10^{-3} - 0.130$	0.001 - 2.692
30	3.736	0.022	0.549
	0.052 - 54.560	$< 10^{-3} - 0.348$	0.008 - 7.249

Results: joint HE EM and GW detections - afterglow emission

Integration Time (s)	EM (yr^{-1})	No latency	
		EM and GW 2016-2017 (yr^{-1})	EM and GW design (yr^{-1})
10	0.12 (0.003 - 1.53)	0.001 ($< 10^{-3}$ - 0.01)	0.02 (0.001 - 0.25)
100	0.20 (0.004 - 2.44)	0.002 ($< 10^{-3}$ - 0.02)	0.04 (0.001 - 0.45)
10^3	0.32 (0.009 - 4.15)	0.003 ($< 10^{-3}$ - 0.05)	0.07 (0.002 - 0.81)
10^4	0.52 (0.02 - 6.64)	0.007 ($< 10^{-3}$ - 0.09)	0.12 (0.004 - 1.36)

Integration Time (s)	EM (yr^{-1})	10 minute latency	
		EM and GW 2016-2017 (yr^{-1})	EM and GW design (yr^{-1})
10	0.002 ($< 10^{-3}$ - 0.05)	$< 10^{-3}$ ($< 10^{-3}$ - 0.01)	$< 10^{-3}$ ($< 10^{-3}$ - 0.04)
100	0.09 (0.003 - 1.17)	0.002 ($< 10^{-3}$ - 0.02)	0.03 (0.001 - 0.37)
10^3	0.30 (0.009 - 3.83)	0.003 ($< 10^{-3}$ - 0.05)	0.07 (0.002 - 0.80)
10^4	0.51 (0.02 - 6.47)	0.007 ($< 10^{-3}$ - 0.09)	0.12 (0.004 - 1.34)

Conclusions

Conclusions

- We have estimated the GW detection rates and sky localizations for NS-NS mergers, finding values consistent with the ones reported in literature
- We have presented estimates of the joint HE EM and GW detection rates with *Fermi*

Next steps

- Extension to NS-BH systems
- Extension of the work to other observatories (X-ray, optical...)
- Use of galaxy catalogs in the simulations
- Public database?

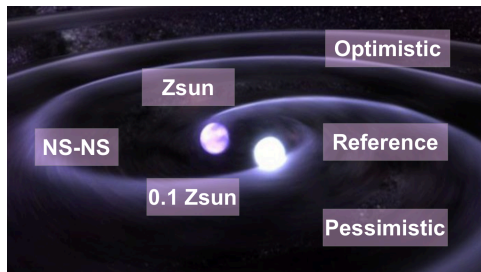
Use of galaxy catalogs

Which galaxy catalogs?

- Good level of completeness
 - Good redshift coverage (at least up to ~ 1 Gpc)
-
- **GLADE** (Dalya et al.)
 - <http://aquarius.elte.hu/glade/index.html>
 - Constructed from four existing galaxy catalogs: GWGC, 2MPZ, 2MASS XSC and HyperLEDA
 - Complete up to ~ 70 Mpc (50 % of completeness at ~ 300 Mpc)
 - **GWENS** (Nissanke et al.)
 - https://astro.ru.nl/catalogs/sdss_gwgalcat/index.html
 - Obtained using SDSS photometric and spectroscopic data
 - Problems within 100 - 200 Mpc, but...
 - ...it extends up to ~ 1 Gpc

Public database?

- Which data?
 - Ascii tables with all simulated NS-NS systems (masses, sky position, distance...) ~ 130 Mb
 - Ascii tables with GW detections (SNR, sky localization area...) ~ 80 Mb
 - Skymaps (fits files) ~ 50 Gb
- VO tools?



Computing resources

Simulations:

- 1000 1-year runs
 - 2 metallicities (Z)
 - 3 theoretical models for each Z
 - 2 GW detector configurations
- ⇒ 12000 realizations

Example

- 1 job
(1 run, Standard Model B,
"2016-2017" configuration)
- CPU time: ~ 2200 s
- elapse time: ~ 1 hour
- Memory usage: ~ 1.5 Gb

Backup slides

Backup slides

GRB afterglow emission - Lorentz factor

Evolution of the Lorentz factor Γ of the shell using an approximate sharp transition from the coasting phase, when

$$\Gamma \sim \Gamma_0$$

to the deceleration phase, when

$$\Gamma(t_{\text{obs}}) = \Gamma_0 (t_{\text{obs}}/t_{\text{dec}})^{-3/8};$$

furthermore, after the jet break we further evolve the Lorentz factor as

$$\Gamma(t_{\text{obs}}) \propto (t_{\text{obs}}/t_j)^{-1/2}$$

(see Sari et al. 1998, Rhoads et al. 1999).

- $\Gamma_0 = 2000$ (Ghirlanda et al. 2010, Ghisellini et al. 2010)
- $t_{\text{dec}} \sim 0.3$ s, corresponding to t_{peak} (see also De Pasquale et al. 2010, Corsi et al. 2010)

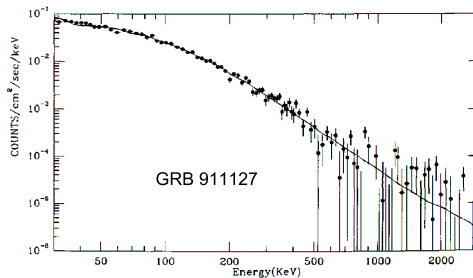
$$\rightarrow t_{\text{dec}}^{\text{sim}} = t_{\text{dec}} \times \frac{1+z}{1+z_0}$$

- $t_j \sim 2 \cdot 10^3$ s (Panaitescu et al. 2010)

$$\rightarrow t_j^{\text{sim}} = t_j \times \frac{(1+z)(\theta + \theta_j)^{8/3}}{(1+z_0)\theta_j^{8/3}}$$

The Band function

$$N_E(E) = \begin{cases} A \left(\frac{E}{100\text{keV}}\right)^\alpha \exp\left(-\frac{E}{E_0}\right) & (\alpha - \beta)E_0 \geq E \\ A \left[\frac{(\alpha - \beta)E_0}{100\text{keV}}\right]^{(\alpha - \beta)} \exp(\beta - \alpha) \left(\frac{E}{100\text{keV}}\right)^\beta & (\alpha - \beta)E_0 \leq E \end{cases}$$



Band et al. (1993)